

Long-Lived Qubit Memory Using Atomic Ions

C. Langer,* R. Ozeri, J. D. Jost, J. Chiaverini, B. DeMarco,† A. Ben-Kish,‡ R. B. Blakestad, J. Britton, D. B. Hume, W. M. Itano, D. Leibfried, R. Reichle, T. Rosenband, T. Schaetz,§ P. O. Schmidt,|| and D. J. Wineland

National Institute of Standards and Technology, 325 Broadway, Boulder, Colorado 80305, USA

(Received 9 April 2005; published 2 August 2005)

We demonstrate experimentally a robust quantum memory using a magnetic-field-independent hyperfine transition in ${}^9\text{Be}^+$ atomic ion qubits at a magnetic field $B \approx 0.01194$ T. We observe that the single physical qubit memory coherence time is greater than 10 s, an improvement of approximately 5 orders of magnitude from previous experiments with ${}^9\text{Be}^+$. We also observe long coherence times of decoherence-free subspace logical qubits comprising two entangled physical qubits and discuss the merits of each type of qubit.

DOI: 10.1103/PhysRevLett.95.060502

PACS numbers: 03.67.Pp, 03.65.Yz, 03.67.Mn, 32.60.+i

Scalable quantum information processing (QIP) requires physical systems capable of reliably storing coherent superpositions for periods over which quantum error correction can be implemented [1]. Moreover, suppressing memory error rates to very low levels allows for simpler error-correcting algorithms [2,3]. In many current atomic ion QIP experiments, a dominant source of memory error is decoherence induced by fluctuating ambient magnetic fields [4,5]. To address this problem, we investigate creating long-lived qubit memories using a first-order magnetic-field-independent hyperfine transition and logical qubits of a decoherence-free subspace (DFS) [6].

Atomic systems have proven themselves as good candidates for quantum information storage through their use in highly stable atomic clocks [7]. Here, the principle of using first-order magnetic-field-independent transitions is well established. A typical clock transition $|F, m_F = 0\rangle \leftrightarrow |F', m_{F'} = 0\rangle$ between hyperfine states of angular momentum F and F' in alkali atoms has no linear Zeeman shift at zero magnetic field, and coherence times exceeding 10 min have been observed [8]. Unfortunately, the degeneracy of magnetic sublevels at zero magnetic field makes it more advantageous to operate at a nonzero field in order to spectrally resolve the levels, thereby inducing a linear field dependence of the transition frequency. However, field-independent transitions between hyperfine states also exist at nonzero magnetic field. For example, coherence times exceeding 10 min have been observed in ${}^9\text{Be}^+$ ions at a magnetic field $B \approx 0.8194$ T [9].

In neutral-atom systems suitable for QIP, field-independent transitions at nonzero magnetic field have been investigated in rubidium [10,11]. The radio-frequency (rf)/microwave two-photon hyperfine transition $|F = 1, m_F = -1\rangle \leftrightarrow |F' = 2, m_{F'} = 1\rangle$ is field-independent at approximately 3.23×10^{-4} T, and coherence times of 2.8 s have been observed [11]. In these and the clock experiments, transitions were driven by microwave fields on large numbers of atoms. Using microwaves, it may be difficult to localize the fields well enough to drive

individual qubits unless a means (e.g., a magnetic-field gradient or Stark-shift gradient) is employed to provide spectral selection [12,13], a technique that has the additional overhead of keeping track of the phases induced by these shifts. With transitions induced by laser beams, the addressing can be accomplished by strong focusing [5] or by weaker focusing and inducing transitions in separate trap zones [4]. In contrast to microwave fields, optical fields (using appropriate geometry [14,15]) provide stronger field gradients that are desirable for coupling ion motional states with internal states, a requirement for certain universal multiqubit logic gates [14,16]. Here, we explore the coherence time of a single atomic ion qubit in a scalable QIP architecture using laser beam addressing.

In recent ${}^9\text{Be}^+$ QIP experiments utilizing $2s\ 2S_{1/2}$ hyperfine states: $|F = 2, m_F = -2\rangle$ and $|F = 1, m_F = -1\rangle$ as qubit levels, fluctuating ambient magnetic fields caused significant decoherence [4,17]. There, the qubit transition depended linearly on the magnetic field with a coefficient of approximately 21 kHz/ μT (Fig. 1). Thus, random mag-

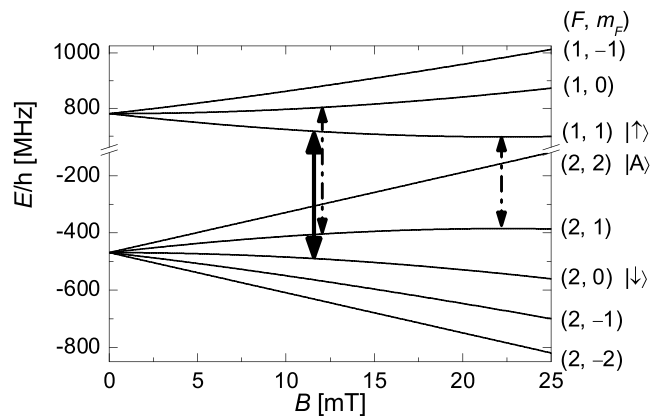


FIG. 1. Hyperfine level structure of the $2s\ 2S_{1/2}$ state of ${}^9\text{Be}^+$. The solid arrow indicates the magnetic-field-independent transition studied here (0.01194 T); the dashed arrows indicate other useful field-independent transitions at 0.01196 T and 0.02231 T.

netic field changes of $0.1 \mu\text{T}$ (typical in our laboratories) would dephase qubit superpositions (to a phase uncertainty of 1 rad) in $80 \mu\text{s}$. To mitigate this decoherence, refocusing spin-echo π pulses were inserted in the experimental sequences [4,17] to limit the bandwidth of noise to which the qubits were susceptible. However, these effects could not be eliminated completely, and fluctuating fields remained a major source of error in these experiments.

The energy spectrum of the ground hyperfine states of ${}^9\text{Be}^+$ as a function of magnetic field is shown in Fig. 1. At $B_0 \approx 0.01194 \text{ T}$, the transition $|F = 2, m_F = 0\rangle \equiv |\downarrow\rangle \leftrightarrow |F = 1, m_F = 1\rangle \equiv |\uparrow\rangle$ (frequency $\nu_{\uparrow\downarrow} \approx 1.2 \text{ GHz}$) is first-order field independent with second-order dependence given by $(0.305 \text{ Hz}/\mu\text{T}^2)(B - B_0)^2$. Given random magnetic-field changes of $0.1 \mu\text{T}$, we expect superpositions of $|\downarrow\rangle$ and $|\uparrow\rangle$ to dephase in approximately 50 s. The transition $|F = 2, m_F = 2\rangle \equiv |A\rangle \leftrightarrow |\uparrow\rangle$ (frequency $\nu_{\uparrow A} \approx 1.0 \text{ GHz}$) is first-order field sensitive with linear dependence of $17.6 \text{ kHz}/\mu\text{T}$ for $B = B_0$. We use frequency measurements of this transition as a probe of the magnetic field. We note that the $|F = 2, m_F = 1\rangle \leftrightarrow |F' = 1, m_{F'} = -1\rangle$ transition, similar to that in Rb [10,11], is field independent in ${}^9\text{Be}^+$ at $B \approx 2.54 \times 10^{-5} \text{ T}$; however, using detuned laser excitation fields, this transition is less practical as it is a four-photon transition.

In the experiment, a single ${}^9\text{Be}^+$ ion is confined to a zone of a trap similar to that in Ref. [18]. The ion is optically pumped to the state $|A\rangle$, and its motion is Doppler cooled by use of the cycling transition $|A\rangle \leftrightarrow |2p^2P_{3/2}, F' = 3, m_{F'} = 3\rangle$ [15]. We detect the state of the ${}^9\text{Be}^+$ ion through state-dependent resonance fluorescence on the cycling transition ($|A\rangle$ fluoresces strongly, whereas the other states do not). Using coherent rotations described below, we measure the $|\downarrow\rangle$, $|\uparrow\rangle$ ‘‘qubit’’ level populations by mapping the states $|\uparrow\rangle$ and $|\downarrow\rangle$ to $|A\rangle$ and $|\uparrow\rangle$, respectively, and measuring the state $|A\rangle$.

Coherent rotations between states $|A\rangle \leftrightarrow |\uparrow\rangle$ and $|\uparrow\rangle \leftrightarrow |\downarrow\rangle$ have the form (in the Bloch sphere representation)

$$R(\theta, \phi) = \cos\frac{\theta}{2}I - i\sin\frac{\theta}{2}\cos\phi\sigma_x - i\sin\frac{\theta}{2}\sin\phi\sigma_y, \quad (1)$$

where I is the identity matrix, σ_i are Pauli operators, θ is the rotation angle, and ϕ is the angle from the x axis to the rotation axis (in the x - y plane). These rotations are driven by two-photon stimulated Raman transitions using focused laser beams [15,16]. We modulate one polarization component of a single laser beam with an electro-optic modulator. This technique simplifies the stabilization of differential optical path length fluctuations between the two Raman beams (generated by the two polarizations), similar to Ref. [19]. The difference in optical path, due to the static birefringence of the modulator, is stabilized to its optimal value of $\lambda/4$ by measuring the retardation with an optical phase detector and feeding back on the temperature of an additional birefringent crystal in the beam path.

To characterize the field-independent transition, we perform Ramsey spectroscopy [20] on the two transitions $|A\rangle \leftrightarrow |\uparrow\rangle$ and $|\downarrow\rangle \leftrightarrow |\uparrow\rangle$ for different magnetic fields (Fig. 2). The magnetic field is determined from the $\nu_{\uparrow A}$ measurement. By measuring $\nu_{\uparrow\downarrow}$ at $B = B_0$ for different rf trapping strengths and extrapolating to zero, we can determine the corresponding ac Zeeman shift produced by the trap’s rf currents. This shift [1.81(2) Hz] was removed from the data in Fig. 2. The calculated solid curve in Fig. 2 is derived from data in Refs. [9,21].

We measure the qubit coherence time by adjusting the magnetic field to the minimum of Fig. 2 and performing Ramsey spectroscopy on the $|\downarrow\rangle \leftrightarrow |\uparrow\rangle$ transition for different Ramsey intervals T_R . The ${}^9\text{Be}^+$ ion is first Doppler cooled and prepared in the state $|\uparrow\rangle$. We then apply the rotation $R(\frac{\pi}{2}, 0)$, creating the superposition state $|\Psi_1\rangle = \frac{1}{\sqrt{2}}(|\uparrow\rangle - i|\downarrow\rangle)$ and wait for the Ramsey interval T_R during which the state evolves to $|\Psi_2\rangle = \frac{1}{\sqrt{2}}(e^{i\phi_D}|\uparrow\rangle - i|\downarrow\rangle)$. The phase ϕ_D is given by the integrated detuning of the (well-controlled) Raman beams’ frequency difference from the qubit transition frequency over the Ramsey interval T_R . A second rotation $R(\frac{\pi}{2}, \phi)$ is then applied with ϕ variable. Repeating the experiment many times and performing a projective measurement of the state $|\uparrow\rangle$ as described above yields

$$P_{\uparrow} = \frac{1}{2}[1 - \cos(\phi_D + \phi)], \quad (2)$$

the probability of measuring the state $|\uparrow\rangle$. The measurement sequence is repeated for different phases ϕ , and the detected probability P_{\uparrow} is fit to the function $f = a - \frac{b}{2} \times \cos(d\phi + \phi_D)$. The fit parameter d allows for magnetic-field drift in time as successive phase points are recorded sequentially; d is close to unity for all scans in this data set. Phase scans for $T_R = 4 \text{ ms}$ and 4 s are shown in Fig. 3(a). Any fluctuation in ϕ_D during the Ramsey interval T_R will

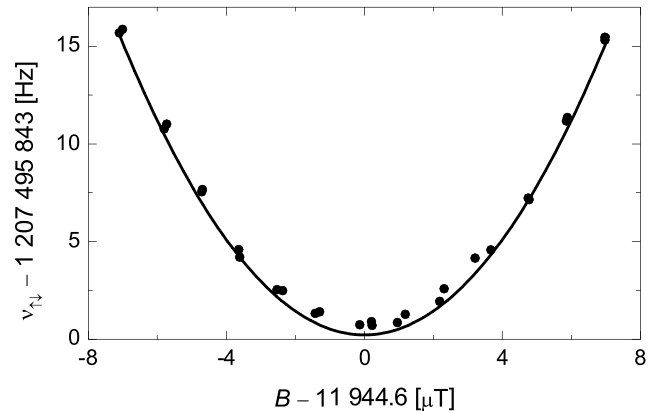


FIG. 2. Frequency of the field-independent transition $|\downarrow\rangle \leftrightarrow |\uparrow\rangle$ as a function of magnetic field. Circles are measured data points; the solid curve is a theoretical prediction. The statistical uncertainty of each datum is $\Delta B \approx 3 \text{ nT}$ and $\Delta\nu_{\uparrow\downarrow} \approx 0.3 \text{ Hz}$.

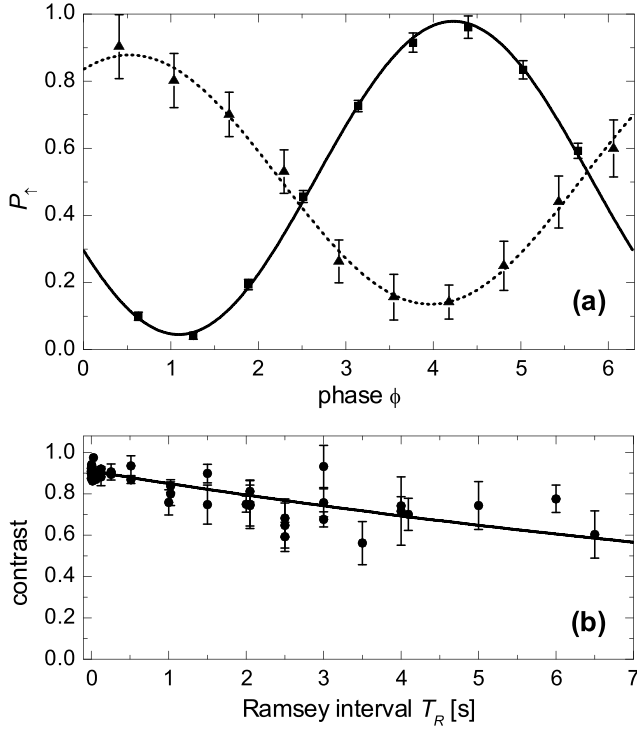


FIG. 3. (a) Ramsey data at $T_R = 4$ ms (squares) and 4 s (triangles). The y axis represents the probability of measuring the state $|\uparrow\rangle$. The contrast b for the 4 ms data is 0.933 ± 0.014 and for the 4 s data is 0.742 ± 0.043 . The $\phi_D \approx 1$ rad phase shift in the 4 ms data is due to detuning the local oscillator by the differential Stark shift (~ 4.2 kHz) such that the Ramsey $\pi/2$ pulses are resonant. (b) Contrast vs Ramsey interval T_R . Each datum represents the fitted contrast b for a phase scan with Ramsey interval T_R . The solid curve is a weighted least-squares fit to the data with reduced $\chi^2 \approx 1.16$.

reduce the contrast b . The form of contrast decay vs T_R is dependent on the spectrum of magnetic-field noise which has components corresponding to times both long and short compared to T_R . The coherence time is limited in part by slow drift of the magnetic field over the measurement time scale of a single point. For the $T_R = 4$ s data in Fig. 3(a), this time scale is 400 s. Moreover, since the measurement of the contrast can take many hours for the longer Ramsey intervals, the magnetic noise environment can vary over different points in Fig. 3(b). As a benchmark, we fit the contrast b for different T_R to the exponential $b(T_R) = b_0 e^{-T_R/\tau}$ [Fig. 3(b)] and find $\tau = 14.7 \pm 1.6$ s. In principle, if the magnetic-field drift is small for the period of a single measurement, we can interrupt data collection to measure (via ν_{1A}) and correct for magnetic-field deviations from B_0 .

Logical qubits of the DFS [6] comprising two entangled physical qubits in the form of Bell states,

$$|\Psi_{\pm}\rangle = \frac{1}{\sqrt{2}}(|01\rangle \pm |10\rangle), \quad (3)$$

are also immune to fluctuations in (uniform) magnetic fields. Any phase acquired due to a fluctuation of magnetic field by one state of the superposition is acquired equally by the other state of the superposition. In the experiment described below (performed in a separate but similar trap), the physical qubit states $|0\rangle$ and $|1\rangle$ are the magnetic-field-sensitive hyperfine states $|F = 1, m_F = -1\rangle$ and $|F = 2, m_F = -2\rangle$ respectively at a field $B \approx 0.0013$ T. Using the technique of Ref. [22], we demonstrate that entanglement is long lived.

Even though the states $|\Psi_{\pm}\rangle$ are immune to uniform time-varying magnetic fields, they are *not* invariant to magnetic-field differences between the locations of the two ions. Such a gradient can cause the states $|01\rangle$ and $|10\rangle$ to acquire phase at a differential rate $\Delta\phi(t)$ due to the different local magnetic fields. This results in a coherent oscillation between $|\Psi_+\rangle$ and $|\Psi_-\rangle$ according to

$$|\psi(t)\rangle = \cos\left[\frac{\Delta\phi(t)}{2}\right]|\Psi_+\rangle + i \sin\left[\frac{\Delta\phi(t)}{2}\right]|\Psi_-\rangle. \quad (4)$$

Before each experiment we perform Doppler cooling, resolved-sideband cooling, and optical pumping to bring the two ions to the vibrational ground state in the trap with internal state $|11\rangle$ [23]. As described in [24], we prepare the maximally entangled state

$$|\Phi_{-i}\rangle = \frac{1}{\sqrt{2}}(|00\rangle - i|11\rangle). \quad (5)$$

Following this step, we apply a rotation $R(\frac{\pi}{2}, -\frac{\pi}{4})$ to both ions to create the state, $|\Psi_+\rangle$.

After preparation of the $|\Psi_+\rangle$ state, we wait for a delay t_D and then apply a final rotation $R(\frac{\pi}{2}, 0)$ to both qubits. This transforms $|\Psi_+\rangle$ into the Bell state $|\Phi_+\rangle = \frac{1}{\sqrt{2}}(|00\rangle + |11\rangle)$, but does not affect the singlet state $|\Psi_-\rangle$ as it is invariant under collective rotations. We detect both ions simultaneously; from the fluorescence count distributions, we can determine the parity of the final state [25] and therefore the probabilities of $|\Psi_+\rangle$ and $|\Psi_-\rangle$ in Eq. (4) as a function of t_D .

Figure 4 displays data for the coherent oscillation around three different delays t_D . For these data, the magnetic-field gradient induces an oscillation frequency

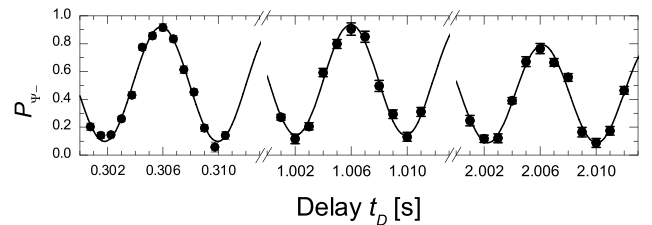


FIG. 4. Coherent oscillation between $|\Psi_+\rangle$ and $|\Psi_-\rangle$ states as a function of delay t_D . P_{Ψ_-} represents the probability of measuring $|\Psi_-\rangle$. The line is a sinusoidal fit to the data. Data are shown after delays of 300 ms, 1 s, and 2 s.

of approximately 125 Hz. From the decay of the $|\Psi_+\rangle$, $|\Psi_-\rangle$ oscillations with delay t_D we extract a Bell-state lifetime of 7.3 ± 1.6 s, assuming exponential decay (reduced $\chi^2 \approx 1.62$). The measured entanglement lifetime was limited by fluctuations in the magnetic-field gradient whose spectrum we have not characterized.

Combining field-independent qubits and DFS states, we could create memories even more robust than the DFS Bell states demonstrated here and in Ref. [22], as different local magnetic fields will induce very small frequency shifts of the qubit transition. The other two states in the Bell basis $\frac{1}{\sqrt{2}}(|00\rangle \pm |11\rangle)$ will also benefit from reduced decoherence due to magnetic-field noise.

In summary, we have shown how magnetic-field-independent qubits can serve as good memory elements in a trapped-ion-based quantum information processor. DFS qubits as demonstrated here and in [6,22] can also be used as good memory elements, with the additional overhead of encoding into the DFS states. Combining both techniques should lead to memory elements with extremely long coherence times. One disadvantage of field-independent qubits is that gates relying on differential Stark shifts between the qubit states [24] will cease to work when the qubit transition frequency is small compared to the Raman beam detuning from the excited states, since the Stark shifts of the qubit states will be nearly the same. To overcome this limitation, we can momentarily change the qubit states, perform the gate, and transform back to the original qubit basis. If the ambient magnetic fields fluctuate on time scales much longer than the duration of these three steps, accumulated phase errors should be negligible. Alternatively, we could apply a gate in which both bits are simultaneously flipped [26–28].

The demonstration of robust qubit memories and long-lived entanglement in trapped atomic ion systems satisfies one of the requirements necessary for large scale quantum information processing. Assuming exponential decay, the probability of memory error is 1.4×10^{-5} for current detection durations of 200 μ s, which is below the fault-tolerant thresholds set by Steane [2] and Knill [29]. This, in combination with the ability to reduce spontaneous emission errors during laser excitation [30], makes atomic ion systems promising candidates for fault-tolerant QIP.

The authors thank Jeroen Koelemeij, Signe Seidelin, and Emanuel Knill for helpful discussion. This work was supported by the US National Security Agency (NSA) and the

Advanced Research and Development Activity (ARDA) under contract no. MOD-7171.05. This manuscript is a publication of NIST and is not subject to U.S. copyright.

*Electronic address: clanger@boulder.nist.gov

†Present address: University of Illinois at Urbana-Champaign

‡Present address: Technion, Israel

§Present address: Max Planck Institute of Quantum Optics

||Present address: University of Innsbruck, Austria

- [1] J. Preskill, Proc. R. Soc. A **454**, 385 (1998).
- [2] A. M. Steane, Phys. Rev. A **68**, 042322 (2003).
- [3] E. Knill, R. Laflamme, and W. H. Zurek, Proc. R. Soc. A **454**, 365 (1998).
- [4] M. D. Barrett *et al.*, Nature (London) **429**, 737 (2004).
- [5] M. Riebe *et al.*, Nature (London) **429**, 734 (2004).
- [6] D. Kielpinski *et al.*, Science **291**, 1013 (2001).
- [7] S. A. Diddams *et al.*, Science **306**, 1318 (2004).
- [8] P. T. H. Fisk *et al.*, IEEE Trans. Instrum. Meas. **44**, 113 (1995).
- [9] J. J. Bollinger *et al.*, IEEE Trans. Instrum. Meas. **40**, 126 (1991).
- [10] D. M. Harber *et al.*, Phys. Rev. A **66**, 053616 (2002).
- [11] P. Treutlein *et al.*, Phys. Rev. Lett. **92**, 203005 (2004).
- [12] F. Mintert and C. Wunderlich, Phys. Rev. Lett. **87**, 257904 (2001).
- [13] D. Schrader *et al.*, Phys. Rev. Lett. **93**, 150501 (2004).
- [14] J. I. Cirac and P. Zoller, Phys. Rev. Lett. **74**, 4091 (1995).
- [15] C. Monroe *et al.*, Phys. Rev. Lett. **75**, 4011 (1995).
- [16] D. J. Wineland *et al.*, J. Res. Natl. Inst. Stand. Technol. **103**, 259 (1998).
- [17] J. Chiaverini *et al.*, Nature (London) **432**, 602 (2004).
- [18] M. A. Rowe *et al.*, Quantum Inf. Comput. **2**, 257 (2002).
- [19] P. J. Lee *et al.*, Opt. Lett. **28**, 1582 (2003).
- [20] N. F. Ramsey, *Molecular Beams* (Oxford University, London, 1963).
- [21] D. J. Wineland, J. J. Bollinger, and W. M. Itano, Phys. Rev. Lett. **50**, 628 (1983).
- [22] C. F. Roos *et al.*, Phys. Rev. Lett. **92**, 220402 (2004).
- [23] B. E. King *et al.*, Phys. Rev. Lett. **81**, 1525 (1998).
- [24] D. Leibfried *et al.*, Nature (London) **422**, 412 (2003).
- [25] M. A. Rowe *et al.*, Nature (London) **409**, 791 (2001).
- [26] K. Mølmer and A. Sørensen, Phys. Rev. Lett. **82**, 1835 (1999).
- [27] C. A. Sackett *et al.*, Nature (London) **404**, 256 (2000).
- [28] P. J. Lee *et al.*, quant-ph/0505203.
- [29] E. Knill, Nature (London) **434**, 39 (2005).
- [30] R. Ozeri *et al.*, Phys. Rev. Lett. **95**, 030403 (2005).